New behaviors of α-particle preformation factors near doubly magic ^{100}Sn*

Jun-Gang Deng(邓军刚)[1,2] Hong-Fei Zhang(张鸿飞)[1,2†] Xiao-Dong Sun(孙小东)[3]

[1]School of Physics, Xi'an Jiaotong University, Xi'an 710049, China
[2]School of Nuclear Science and Technology, Lanzhou University, Lanzhou 730000, China
[3]China Nuclear Data Center, China Institute of Atomic Energy, Beijing 102413, China

Abstract: The α-particle preformation factors of nuclei above doubly magic nuclei ^{100}Sn and ^{208}Pb are investigated within the generalized liquid drop model. The results show that the α-particle preformation factors of nuclei near self-conjugate doubly magic ^{100}Sn are significantly larger than those of analogous nuclei just above ^{208}Pb, and they will be enhanced as the nuclei move towards the $N = Z$ line. The proton–neutron correlation energy E_{p-n} and two protons–two neutrons correlation energy E_{2p-2n} of nuclei near ^{100}Sn also exhibit a similar situation, indicating that the interactions between protons and neutrons occupying similar single-particle orbitals could enhance the α-particle preformation factors and result in superallowed α decay. This also provides evidence of the significant role of the proton–neutron interaction on α-particle preformation. Also, the linear relationship between α-particle preformation factors and the product of valence protons and valence neutrons for nuclei around ^{208}Pb is broken in the ^{100}Sn region because the α-particle preformation factor is enhanced when a nucleus near ^{100}Sn moves towards the $N = Z$ line. Furthermore, the calculated α decay half-lives fit well with the experimental data, including the recent observed self-conjugate nuclei ^{104}Te and ^{108}Xe [Phys. Rev. Lett. 121, 182501 (2018)].

Keywords: α decay, α-particle preformation factor, doubly magic nucleus, generalized liquid drop model

DOI: 10.1088/1674-1137/ac5a9f

α decay is a fundamental nuclear decay mode. Research on α decay has long been focused in the vicinities of doubly magic nuclei ^{208}Pb ($Z = 82$, $N = 126$) and ^{298}Fl ($Z = 114$, $N = 184$) because α decay can be a probe to study unstable nucleus structures, and can be the only way to identify new synthesized superheavy nuclei [1–27]. Over the past two decades, α emitters around the self-conjugate doubly magic nucleus ^{100}Sn ($Z = N = 50$) at the opposite end of the mass table have also received a lot of attention and become a hot topic in nuclear physics [18, 28–35]. In particular, there is the fastest α emitter ^{104}Te near doubly magic nucleus ^{100}Sn [34]. Since the α emitters near self-conjugate doubly magic nucleus ^{100}Sn are close to the $N = Z$ line, the nuclear force is extremely sensitive to isospin. Therefore, it is a great chance to study the unique neutron-deficient nuclear structure and examine various α decay theoretical models. Moreover, cluster radioactivity was also predicted as one of the decay modes of nuclei in the ^{100}Sn region [36–39]. Further interest in the decay rates of nuclei around doubly magic nucleus ^{100}Sn comes from research into astrophysical processes, for which this region has been considered as the end of the rapid proton capture process due to the Sn–Sb–Te cycle [33, 40, 41].

In addition, in the neutron-deficient Te, Xe, and Ba isotopes near ^{100}Sn, one would expect that interactions between protons and neutrons occupying similar single-particle orbitals could enhance the α-particle preformation factors, and together with the significantly reduced α-widths compared to the analogous nuclei just above doubly magic nucleus ^{208}Pb, can result in the so-called "superallowed" α decay [42]. This effect would be expected to be strongest for $N = Z$ self-conjugate nuclei [42]. Recently, α radioactivity to a heavy self-conjugate nucleus was observed for the first time on the ^{108}Xe$\rightarrow$^{104}Te$\rightarrow$^{100}Sn α decay chain [34], including the measurements of the α-particle kinetic energy and α decay half-lives of the α emitters ^{108}Xe [$E_\alpha = 4.4(2)$ MeV, $T_{1/2} = 58^{+106}_{-23}$ μs] and ^{104}Te [$E_\alpha = 4.9(2)$ MeV, $T_{1/2} < 18$ ns]. The authors of this article suggested that the α-reduced width for ^{108}Xe or ^{104}Te is more than a factor of 5 larger than that for ^{212}Po [34].

It is well known that ^{104}Te, near the proton drip line, and ^{212}Po, near the β–stability line, are the only two existing α emitters decaying to doubly magic nuclei. In recent years, researchers adopted different models such as the density dependent cluster model (DDCM) [28,

Received 6 December 2021; Accepted 7 March 2022; Published online 6 May 2022

* Supported by the National Natural Science Foundation of China (12175170, 11675066, 12005303)

† E-mail: zhanghf@xjtu.edu.cn

43–45], the generalized liquid drop model (GLDM) [46, 47], the preformed cluster model (PCM) [48], etc. to study the α decay of nuclei around doubly magic ^{208}Pb and ^{100}Sn, and provide some important insights on the α-particle preformation factor. In this letter, we focus on the α-particle preformation factors of nuclei near self-conjugate doubly magic nucleus ^{100}Sn, and compare them to those of analogous nuclei just above the doubly magic nucleus ^{208}Pb, based on the available experimental data of α decay [34, 49–59] within the generalized liquid drop model (GLDM) [60–66]. These α emitters have different isospins and mass numbers as well as different proton and neutron closed shells. We want to reveal some new behaviors of α-particle preformation factors for extremely neutron-deficient nuclei near self-conjugate doubly magic nucleus ^{100}Sn, in order to understand the roles of proton–neutron correlation and the single-particle orbitals occupied by protons and neutrons in the preformation of α-clusters, as well as the physical mechanism of superallowed α decay.

The GLDM can deal well with proton radioactivity [67], cluster radioactivity [68], fusion [69], fission [70], and the α decay process [22, 60–66, 71] by introducing the quasimolecular shape mechanism [60], which can describe the complex deformation process from the parent nucleus through continuous transition to the appearance of a deep and narrow neck, finally resulting in two tangential fragments, and adding the proximity energy, including an accurate radius and mass asymmetry. In previous works [60–66], the GLDM has been introduced in detail. The α decay half-life can be obtained by

$$T_{1/2} = \frac{\ln 2}{\lambda}, \tag{1}$$

with the α decay constant λ being expressed as

$$\lambda = P_\alpha \nu P, \tag{2}$$

where the assault frequency ν is obtained using the classical method with the kinetic energy of the α-particle. The barrier-penetrating probability P is determined by tunneling the GLDM potential barriers [60–66] with the Wentzel–Kramers–Brillouin (WKB) approximation.

The experimental α-particle preformation factor $P_\alpha^{\rm Exp}$ can be extracted from the ratios of the theoretical decay half-life $T_{1/2}^{\rm Cal1}$, calculated by assuming the α-particle preformation factor is a constant $P_\alpha = 1$, to experimental decay half-life [65, 72–75]. This is expressed as

$$P_\alpha^{\rm Exp} = \frac{T_{1/2}^{\rm Cal1}}{T_{1/2}^{\rm Exp}}. \tag{3}$$

To examine the experimental α decay half-life data, the analytic formula for estimating the α-particle preformation factor is also adopted, which was put forward in our previous works [66, 71]. It is expressed as

$$\log_{10} P_\alpha^{\rm Eq} = a + bA^{1/6}\sqrt{Z} + c\frac{Z}{\sqrt{Q_\alpha}} - d\chi' - e\rho' + f\sqrt{l(l+1)}, \tag{4}$$

where

$$\chi' = Z_1 Z_2 \sqrt{\frac{A_1 A_2}{(A_1 + A_2)Q_\alpha}}$$

and

$$\rho' = \sqrt{\frac{A_1 A_2}{A_1 + A_2} Z_1 Z_2 \left(A_1^{1/3} + A_2^{1/3}\right)}.$$

A, Z, and Q_α represent mass number, proton number, and α decay energy of the parent nucleus. A_1, Z_1, A_2, and Z_2 denote the mass and proton numbers of the α-particle and daughter nucleus. l is the angular momentum carried by the α-particle. The parameters values are listed in Ref. [66].

The calculated α decay half-lives for nuclei above doubly magic nuclei ^{100}Sn and ^{208}Pb are presented in Tables 1 and 2, respectively. In these two tables, the first four columns represent the α transition, the experimental kinetic energy of the α-particle, the experimental α decay energy, and the minimum angular momentum carried by the α-particle. The fifth column is the experimental α decay half-life. The sixth column denotes the calculated α decay half-life $T_{1/2}^{\rm Cal1}$ within the GLDM with $P_\alpha = 1$. The seventh column gives the calculated α decay half-life $T_{1/2}^{\rm Cal2}$ within the GLDM with the estimated α-particle preformation factor from Eq. (4). The eighth column shows the extracted experimental α-particle preformation factor by using Eq. (3) with $T_{1/2}^{\rm Cal1}$ and $T_{1/2}^{\rm Exp}$. The last two columns express the calculated proton–neutron correlation energy E_{p-n} and two protons–two neutrons correlation energy E_{2p-2n} determined by Eqs. (6) and (7). From these two tables, it can be seen immediately that the calculated α decay half-lives $T_{1/2}^{\rm Cal2}$ can accurately reproduce the experimental data including the newly observed self-conjugate nuclei ^{104}Te and ^{108}Xe [34]. Note that the calculations provide support for recent experimental observation data in Ref. [34]. In Table 1, for ^{110}Te, the calculated α-particle preformation factor using Eq. (4) is an order of magnitude larger than the extracted value from the experimental α decay half-life data. This is because the α decay branch ratio of ^{110}Te is very small, only 0.00067% [28], and the microscopic calculation of the α-particle preformation factor is very complicated, while Eq. (4)

Table 1. Calculations of α-particle preformation factor, α decay half-lives, and the proton–neutron correlation energy E_{p-n} and two protons–two neutrons correlation energy E_{2p-2n} of even–even Te, Xe, and Ba isotopes near ^{100}Sn.

α transition	E_α/MeV	Q_α/MeV	$l_{\min}$	$T_{1/2}^{\rm Exp}$/s	$T_{1/2}^{\rm Cal1}$/s	$T_{1/2}^{\rm Cal2}$/s	$P_\alpha^{\rm Exp}$	E_{p-n}/MeV	E_{2p-2n}/MeV
^{104}Te→^{100}Sn	4.9 [34]	5.1	0	$<1.80\times10^{-8}$ [34]	1.47×10^{-8}	7.29×10^{-8}	>0.81	1.26[a]	3.64[a]
^{106}Te→^{102}Sn	4.128 [51]	4.29	0	7.00×10^{-5} [50–52]	2.52×10^{-5}	8.38×10^{-5}	0.36	0.56[b]	1.84[a]
^{108}Te→^{104}Sn	3.314 [54]	3.44	0	4.30×10^{0} [51, 53, 54]	9.30×10^{-1}	1.68×10^{0}	0.22	1.06[b]	1.83[b]
^{110}Te→^{106}Sn	2.624 [55]	2.72	0	2.78×10^{6} [55, 56]	3.32×10^{5}	2.87×10^{5}	0.12	0.71[b]	1.73[b]
^{108}Xe→^{104}Te	4.32 [34, 49]	4.49	0	5.80×10^{-5} [34]	3.70×10^{-5}	1.10×10^{-4}	0.64	1.10[a]	3.35[a]
^{110}Xe→^{106}Te	3.72 [50]	3.86	0	1.48×10^{-1} [50]	5.00×10^{-2}	1.07×10^{-1}	0.34	0.73[b]	2.02[a]
^{112}Xe→^{108}Te	3.216 [51]	3.34	0	3.38×10^{2} [51, 53]	1.01×10^{2}	1.53×10^{2}	0.30	1.13[b]	1.66[b]
^{114}Ba→^{110}Xe	3.48 [50]	3.61	0	4.20×10^{1} [50]	2.60×10^{1}	4.19×10^{1}	0.62	0.66[b]	1.96[a]

[a] Calculated by using nuclear mass data in the WS4+ mass model [76]. [b] Calculated using nuclear mass data in the evaluated atomic mass table AME2016 [58, 59].

Table 2. Same as Table 1, but for even–even Po, Rn, and Ra isotopes near ^{208}Pb. The experimental α decay half-lives are taken from the evaluated nuclear properties table NUBASE2016 [57]. The experimental α decay energy are taken from the evaluated atomic mass table AME2016 [58, 59]. The E_{p-n} and E_{2p-2n} energies are calculated using the nuclear mass data in the AME2016 [58, 59].

α transition	E_α/MeV	Q_α/MeV	$l_{\min}$	$T_{1/2}^{\rm Exp}$/s	$T_{1/2}^{\rm Cal1}$/s	$T_{1/2}^{\rm Cal2}$/s	$P_\alpha^{\rm Exp}$	E_{p-n}/MeV	E_{2p-2n}/MeV
^{212}Po→^{208}Pb	8.79	8.95	0	2.95×10^{-7}	1.00×10^{-8}	1.48×10^{-7}	0.03	0.87	1.44
^{214}Po→^{210}Pb	7.69	7.83	0	1.64×10^{-4}	1.14×10^{-5}	1.23×10^{-4}	0.07	0.70	1.28
^{216}Po→^{212}Pb	6.78	6.91	0	1.45×10^{-1}	1.39×10^{-2}	1.09×10^{-1}	0.10	0.51	1.11
^{218}Po→^{214}Pb	6.00	6.12	0	1.86×10^{2}	1.93×10^{1}	1.09×10^{2}	0.10	0.38	1.09
^{212}Rn→^{208}Po	6.26	6.38	0	1.43×10^{3}	1.40×10^{1}	6.86×10^{2}	0.01	0.23	0.57
^{214}Rn→^{210}Po	9.04	9.21	0	2.70×10^{-7}	1.08×10^{-8}	1.85×10^{-7}	0.04	0.67	1.24
^{216}Rn→^{212}Po	8.05	8.20	0	4.50×10^{-5}	4.99×10^{-6}	6.56×10^{-5}	0.11	0.70	1.33
^{218}Rn→^{214}Po	7.13	7.26	0	3.38×10^{-2}	4.23×10^{-3}	4.15×10^{-2}	0.13	0.58	1.29
^{220}Rn→^{216}Po	6.29	6.41	0	5.56×10^{1}	8.33×10^{0}	5.92×10^{1}	0.15	0.52	1.18
^{222}Rn→^{218}Po	5.49	5.59	0	3.30×10^{5}	5.71×10^{4}	2.79×10^{5}	0.17	0.51	1.15
^{214}Ra→^{210}Rn	7.14	7.27	0	2.44×10^{0}	3.25×10^{-2}	1.53×10^{0}	0.01	0.22	0.65
^{216}Ra→^{212}Rn	9.35	9.53	0	1.82×10^{-7}	8.41×10^{-9}	1.70×10^{-7}	0.05	0.52	1.14
^{218}Ra→^{214}Rn	8.39	8.55	0	2.52×10^{-5}	2.44×10^{-6}	3.88×10^{-5}	0.10	0.58	1.21
^{220}Ra→^{216}Rn	7.45	7.59	0	1.79×10^{-2}	1.93×10^{-3}	2.34×10^{-2}	0.11	0.68	1.35
^{222}Ra→^{218}Rn	6.56	6.68	0	3.36×10^{1}	4.46×10^{0}	3.92×10^{1}	0.13	0.44	1.34
^{224}Ra→^{220}Rn	5.69	5.79	0	3.14×10^{5}	4.97×10^{4}	2.99×10^{5}	0.16	0.41	1.25
^{226}Ra→^{222}Rn	4.78	4.87	0	5.05×10^{10}	1.10×10^{10}	4.00×10^{10}	0.22	0.40	1.23

mainly considers the α decay energy, proton number, and mass number when calculating the α-particle preformation factor. This leads to a deviation between the theoretically calculated α-particle preformation factors and the experimental data for nuclei with extremely low α decay branch ratios such as ^{110}Te.

To measure the agreement between the calculated α decay half-lives $T_{1/2}^{\rm Cal2}$ and experimental data $T_{1/2}^{\rm Exp}$, the standard deviations are calculated by

$$\sigma=\sqrt{\tfrac{1}{n}\textstyle\sum(\log_{10}T_{1/2}^{\rm Cal2}-\log_{10}T_{1/2}^{\rm Exp})^2}. \quad (5)$$

For nuclei in Tables 1 and 2, the results of standard deviations $\sigma_1=0.47$ and $\sigma_2=0.16$ are satisfactory, showing that $T_{1/2}^{\rm Cal2}$ can accurately reproduce $T_{1/2}^{\rm Exp}$ within factors of $10^{0.47}=2.95$ and $10^{0.16}=1.45$, respectively. This demonstrates that the GLDM can be applied to extract the experimental α-particle preformation factors for studying the structure information of nuclei in these two regions.

Furthermore, Tables 1 and 2 show that the extracted experimental α-particle preformation factors $P_\alpha^{\rm Exp}$ of nuclei near ^{100}Sn are larger than $P_\alpha^{\rm Exp}$ of nuclei near ^{208}Pb, and in particular, larger than $P_\alpha^{\rm Exp}$ of analogous nuclei just above ^{208}Pb. The analogous nuclei refer to the two nuclei with the same valence proton and valence neutron located above doubly magic cores ^{100}Sn and ^{208}Pb, respectively. The valence protons N_p and valence neutrons N_n are defined as $N_p = Z - Z_0$ and $N_n = N - N_0$ with $Z_0 = 50$ and 82, $N_0 = 50$ and 126, being the magic numbers of protons and neutrons in the corresponding nuclear region. For example, ^{104}Te is analogous to ^{212}Po because they both have two valence protons and two valence neutrons outside of the doubly magic nuclei ^{100}Sn and ^{208}Pb, respectively.

The extracted experimental α-particle preformation factors $P_\alpha^{\rm Exp}$ for nuclei above ^{100}Sn and for analogous nuclei just above ^{208}Pb are shown as functions of valence protons and valence neutrons in Fig. 1 (a), (b), and (c), respectively. In this figure, one can see that $P_\alpha^{\rm Exp}$ for nuclei above ^{100}Sn are significantly larger than those of analogous nuclei just above ^{208}Pb. Furthermore, Fig. 1 (a) shows the variations of $P_\alpha^{\rm Exp}$ for Te ($Z = 52$) and Po ($Z = 84$) isotopes, whose valence protons are $N_p = Z - Z_0 = 2$, against valence neutrons N_n. It is clear that for Te isotopes $P_\alpha^{\rm Exp}$ exhibits an increasing trend when the nucleus moves towards the $N = Z$ line, but Po isotopes do not show similar patterns due to the large asymmetry between neutrons and protons. Figure 1 (b) displays the variations of $P_\alpha^{\rm Exp}$ for Xe ($Z = 54$) and Rn ($Z = 86$) isotopes, whose valence protons are $N_p = Z - Z_0 = 4$, against valence neutrons N_n. We find that for Xe isotopes $P_\alpha^{\rm Exp}$ also increases as the nucleus moves towards the $N = Z$ line. However, Rn isotopes still do not show a similar trend of change. Figure 1 (c) plots $P_\alpha^{\rm Exp}$ as a function of valence protons N_p for $N = 58$ and $N = 134$ isotones, whose valence neutrons are $N_n = N - N_0 = 8$. $P_\alpha^{\rm Exp}$ for $N = 58$ isotopes also show an increasing tendency as the nuclei move towards the $N = Z$ line, but this phenomenon does not occur in the analogous $N = 134$ isotopes just above ^{208}Pb. This indicated that $P_\alpha^{\rm Exp}$ is enhanced when a nucleus moves towards the $N = Z$ line, resulting in the superallowed α decay near doubly magic nucleus ^{100}Sn. In recent work, Clark *et al*. adopted a very different model and studied the α-particle preformation factors of nuclei in these two regions [31]. A similar conclusion was obtained, though the α-particle preformation factors of nuclei near doubly magic nuclei ^{100}Sn and ^{208}Pb are in orders of 10^{-2} and 10^{-3}, respectively.

To investigate the effects of the proton–neutron interaction and the two protons–two neutrons interaction on α-particle preformation, we calculate the proton–neutron correlation energy E_{p-n} and two protons–two neutrons correlation energy E_{2p-2n} using

$$\begin{aligned} E_{p-n} =& B(A,Z) + B(A-2,Z-1) \\ & - B(A-1,Z-1) - B(A-1,Z), \end{aligned} \tag{6}$$

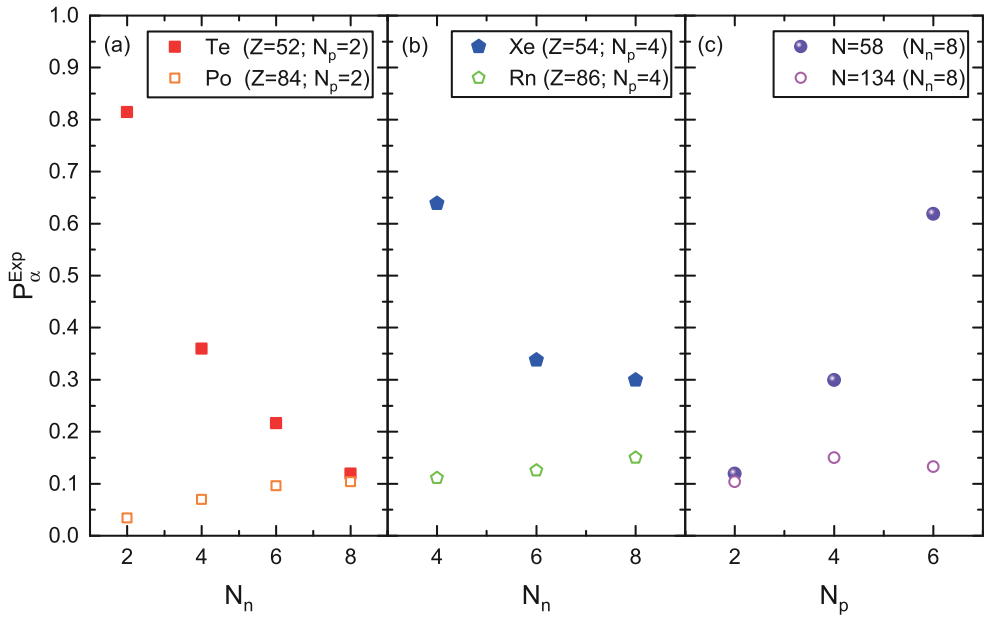

Fig. 1. (color online) Variations of extracted experimental α-particle preformation factors $P_\alpha^{\rm Exp}$ from Eq. (3) against the valence neutrons for $Z = 52$ and $Z = 84$ isotopes (left), and against the valence neutrons for $Z = 54$ and $Z = 86$ isotopes (middle), and against the valence protons for $N = 58$ and $N = 134$ isotones (right), respectively.

$$E_{2p-2n} = B(A,Z) + B(A-4,Z-2) - B(A-2,Z-2) - B(A-2,Z). \quad (7)$$

Equations (6) and (7) were proposed in Ref. [77] and used to determine the experimental pairing energy of the nucleons [78]. $B(A,Z)$ is the binding energy of a nucleus with the mass number A and proton number Z. The results of E_{p-n} energy and E_{2p-2n} energy are listed in the last two columns of Tables 1 and 2. In these two tables, it can be found that the E_{p-n} and E_{2p-2n} energies of nuclei above doubly magic nucleus ^{100}Sn are larger than those of analogous nuclei just above ^{208}Pb. This, in turn, leads to significant enhancement of $P_\alpha^{\rm Exp}$ for nuclei near ^{100}Sn. The results for the E_{p-n} and E_{2p-2n} energies are plotted in Fig. 2. In this figure, the E_{p-n} and E_{2p-2n} energies of nuclei above ^{100}Sn are strengthened when compared to analogous nuclei just above ^{208}Pb. For $Z=52$ isotopes, the E_{p-n} and E_{2p-2n} energies increase rapidly in $N_n=2$. Similarly, for $Z=54$ isotopes, the E_{p-n} and E_{2p-2n} energies rise fast in $N_n=4$. However, the E_{p-n} and E_{2p-2n} energies of analogous nuclei just above ^{208}Pb change slowly. Therefore, it is demonstrated that the α-particle is more likely to form in self-conjugate nuclei, resulting in the superallowed α decay. In addition, the E_{2p-2n} energy appears an increased tendency, the same as $P_\alpha^{\rm Exp}$, when the nucleus moves towards the $N=Z$ line, implying that the two protons–two neutrons interaction plays a more significant role than one proton–one neutron interaction in α-particle preformation.

The extracted experimental α-particle preformation factors $P_\alpha^{\rm Exp}$ for nuclei above ^{100}Sn and ^{208}Pb are shown as functions of $(N_pN_n)/(Z_0+N_0)$ in Fig. 3 (a) and (b), respectively. In Fig. 3 (b), one can see that the closer $(N_pN_n)/(Z_0+N_0)$ is to zero, representing the proton and/or neutron numbers approaching closed shells, the smaller is $P_\alpha^{\rm Exp}$. When $(N_pN_n)/(Z_0+N_0)$ is far from zero, $P_\alpha^{\rm Exp}$ will increase. This indicates that the closer the proton and/or neutron number is to the magic number, the more difficult it is for an α-particle to form inside its par-

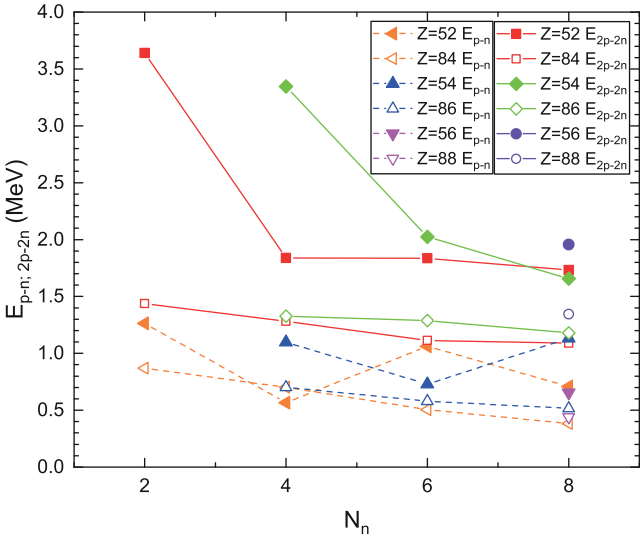

Fig. 2. (color online) Proton–neutron E_{p-n} correlation energy and two protons–two neutrons correlation energy E_{2p-2n} for nuclei above ^{100}Sn (denoted as solid symbols) and analogous nuclei above ^{208}Pb (denoted as open symbols).

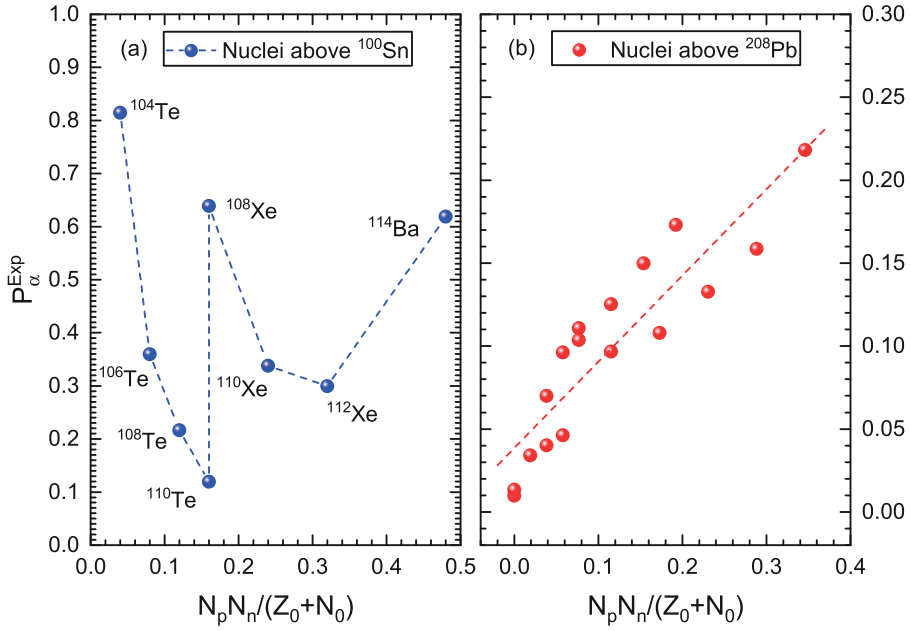

Fig. 3. (color online) Variations of extracted experimental α-particle preformation factors $P_\alpha^{\rm Exp}$ from Eq. (3) against $(N_pN_n)/(Z_0+N_0)$ for nuclei above ^{100}Sn (left) and for nuclei above ^{208}Pb (right).

ent nucleus. We find that $P_\alpha^{\rm Exp}$ is linearly dependent on $(N_pN_n)/(Z_0+N_0)$ for nuclei above ^{208}Pb. This is consistent with the conclusions deduced by adopting different models, in which the α-particle preformation factors are extracted from the ratios between theoretical α decay half-lives calculated by adopting the different models to experimental data [15, 79, 80], or calculated using the differences of binding energy between the α decaying parent nucleus and its neighboring nuclei within the cluster-formation model [81]. It is shown that the nuclear shell effects and the nucleon configurations play key roles in α-cluster preformation for α-particle emitters around doubly magic ^{208}Pb. However, in Fig. 3 (a) this phenomenon is broken in the ^{100}Sn region. The values of $P_\alpha^{\rm Exp}$ for nuclei above ^{100}Sn are linearly independent of $(N_pN_n)/(Z_0+N_0)$ and show a new behavior. When the nucleus is close to shell closure, $P_\alpha^{\rm Exp}$ for nuclei near ^{100}Sn does not decrease like that for nuclei near ^{208}Pb, but rather increases. In addition, we can find that the maximum values of $P_\alpha^{\rm Exp}$ in Fig. 3 (a) correspond to ^{104}Te, ^{108}Xe, and ^{114}Ba. In particular, $P_\alpha^{\rm Exp}$ is significantly enhanced along the $N=Z$ line, which results in $P_\alpha^{\rm Exp}$ for nuclei above ^{100}Sn not being linearly dependent on $(N_pN_n)/(Z_0+N_0)$.

In 2014 and 2017, Wang *et al*. and Seif *et al*. adopted the generalized liquid drop model (GLDM) [46, 47] and the preformed cluster model (PCM) [48], respectively, to study the α decay of even–even, odd-A, and doubly odd nuclei around doubly magic ^{100}Sn. In these works [46–48], the calculated α decay half-lives can accurately reproduce the experimental data, and the α-particle preformation factors evidently depend on the odd–even effect. In addition, in these works [46–48], the calculated α-particle preformation factors of nuclei near doubly magic nucleus ^{100}Sn are of the order of 10^{-1}, larger than ones of nuclei around doubly magic nucleus ^{208}Pb. These works [46–48] also find that the proton–neutron interaction plays an important role in the formation of an α cluster. These important insights support this present work. However, our research further shows that the α-particle preformation factors of nuclei near self-conjugate doubly magic ^{100}Sn are significantly larger than those of analogous nuclei just above ^{208}Pb, and they will be enhanced as the nuclei move towards the $N=Z$ line. Furthermore, our research finds that the linear relationship between α-particle preformation factors and the product of valence protons and valence neutrons for nuclei around ^{208}Pb is broken in the ^{100}Sn region because the α-particle preformation factor is enhanced when the nucleus near ^{100}Sn moves towards the $N=Z$ line.

In general, α decay is approximatively treated as a quasi-stationary-state problem that is characterized by the orbital angular momentum l and the global quantum number G. Based on the Wildermuth rule, the global quantum number $G=2n_r+l$ denotes the principal quantum number with the radial quantum number n_r and angular momentum quantum number l. For α decay [82], G can be obtained by

$$G=2n_r+l=\begin{cases}18, & N\le 82,\\ 20, & 82<N\le 126,\\ 22, & N>126.\end{cases} \tag{8}$$

In the different major proton and neutron closed shells, the different global quantum numbers G describe the different α-core relative motion for α decay near ^{100}Sn and ^{208}Pb, which maybe can also influence the α-particle preformation. In the cluster model [7, 28, 43–45, 82], the quantum effect can be taken into account by the Bohr–Sommerfeld quasiclassical condition. However, the GLDM is a macroscopical model, which doesn't take into account the α-core relative motion. Therefore, the GLDM will need to be improved to introduce the α-core relative motion in the future.

In summary, we have systematically studied the α-particle preformation factors $P_\alpha^{\rm Exp}$ of nuclei above doubly magic nuclei ^{100}Sn and ^{208}Pb, which are extracted from the ratios between the theoretical α-decay half-lives within the GLDM and the experimental data. The results show that $P_\alpha^{\rm Exp}$ for nuclei near self-conjugate doubly magic ^{100}Sn are significantly larger than those of analogous nuclei just above ^{208}Pb, and they will be enhanced when the nucleus moves towards the $N=Z$ line. The proton –neutron correlation energy E_{p-n} and two protons–two neutrons correlation energy E_{2p-2n} for nuclei near ^{100}Sn are also larger than those of analogous nuclei just above ^{208}Pb. This indicates that the interactions between protons and neutrons occupying similar single-particle orbitals could enhance $P_\alpha^{\rm Exp}$ and result in the superallowed α decay near doubly magic nucleus ^{100}Sn. Furthermore, as the nucleus moves towards the $N=Z$ line, the E_{2p-2n} energy shows an increased tendency which is the same as that of $P_\alpha^{\rm Exp}$, while the E_{p-n} energy doesn't follow this pattern, indicating that the E_{2p-2n} energy plays a more important role than E_{p-n} energy in α-particle preformation of superallowed α decay. The linear relationship between $P_\alpha^{\rm Exp}$ and the product of valence protons and valence neutrons $(N_pN_n)/(Z_0+N_0)$ for nuclei above ^{208}Pb is broken in the ^{100}Sn region because $P_\alpha^{\rm Exp}$ is enhanced when the nucleus near ^{100}Sn moves towards the $N=Z$ line. Also, the calculated α decay half-lives can accurately reproduce experimental data including the newly observed self-conjugate nuclei ^{108}Xe and ^{104}Te. This letter also provides evidence of the significant role of the proton –neutron interaction on α-particle preformation, which can shed some new light on α decay and α-particle preformation factors in nuclear physics research in the future.

References

[1] D. F. Geesaman, C. K. Gelbke, R. V. F. Janssens *et al.*, Annu. Rev. Nucl. Part. Sci. **56**(1), 53-92 (2006)
[2] S. Hofmann and G. Münzenberg, Rev. Mod. Phys. **72**, 733-767 (2000)
[3] M. Pfützner, M. Karny, L. V. Grigorenko *et al.*, Rev. Mod. Phys. **84**, 567-619 (2012)
[4] A. N. Andreyev, M. Huyse, P. Van Duppen *et al.*, Phys. Rev. Lett. **110**, 242502 (2013)
[5] L. Ma, Z. Y. Zhang, Z. G. Gan *et al.*, Phys. Rev. C **91**, 051302(R) (2015)
[6] Chong Qi, Roberto Liotta, and Ramon Wyss, Prog. Part. Nucl. Phys. **105**, 214-251 (2019)
[7] B. Buck, A. C. Merchant, and S. M. Perez, Phys. Rev. Lett. **65**, 2975-2977 (1990)
[8] B. Buck, A. C. Merchant, and S. M. Perez, Phys. Rev. Lett. **72**, 1326-1328 (1994)
[9] A. Astier, P. Petkov, M.-G. Porquet *et al.*, Phys. Rev. Lett. **104**, 042701 (2010)
[10] J. W. Beeman, M. Biassoni, C. Brofferio *et al.*, Phys. Rev. Lett. **108**, 062501 (2012)
[11] Pierre de Marcillac, N. Coron, G. Dambier *et al.*, Nature **422**, 876-878 (2003)
[12] Z. Y. Zhang, Z. G. Gan, H. B. Yang *et al.*, Phys. Rev. Lett. **122**, 192503 (2019)
[13] L. Ma, Z. Y. Zhang, Z. G. Gan *et al.*, Phys. Rev. Lett. **125**, 032502 (2020)
[14] M. D. Sun, Z. Liu, T. H. Huang *et al.*, Phys. Lett. B **771**, 303-308 (2017)
[15] W. M. Seif, M. Shalaby, and M. F. Alrakshy, Phys. Rev. C **84**, 064608 (2011)
[16] Yuejiao Ren and Zhongzhou Ren, Phys. Rev. C **85**, 044608 (2012)
[17] Chang Xu, G. Röpke, P. Schuck *et al.*, Phys. Rev. C **95**, 061306(R) (2017)
[18] Shuo Yang, Chang Xu, Gerd Röpke *et al.*, Phys. Rev. C **101**, 024316 (2020)
[19] Zhen Wang, Zhongzhou Ren, and Dong Bai, Phys. Rev. C **101**, 054310 (2020)
[20] Jun-Gang Deng, Hong-Fei Zhang, and G. Royer, Phys. Rev. C **101**, 034307 (2020)
[21] Jun-Gang Deng and Hong-Fei Zhang, Chin. Phys. C **45**(2), 024104 (2021)
[22] Na-Na Ma, Xiao-Jun Bao, and Hong-Fei Zhang, Chin. Phys. C **45**(2), 024105 (2021)
[23] Yi-Bin Qian and Zhong-Zhou Ren, Chin. Phys. C **45**(2), 021002 (2021)
[24] Wei Hua, Zhiyuan Zhang, Long Ma *et al.*, Chin. Phys. C **45**(4), 044001 (2021)
[25] Yan He, Xuan Yu, and Hong-Fei Zhang, Chin. Phys. C **45**(1), 014110 (2021)
[26] Y. Z. Wang, J. M. Dong, B. B. Pengc*et al.*, Phys. Rev. C **81**, 067301 (2010)
[27] Y. Z. Wang, S. J. Wang, Z. Y. Hou *et al.*, Phys. Rev. C **92**, 064301 (2015)
[28] Chang Xu and Zhongzhou Ren, Phys. Rev. C **74**, 037302 (2006)
[29] Monika Patial, R. J. Liotta, and R. Wyss, Phys. Rev. C **93**, 054326 (2016)
[30] Y. Xiao, S. Go, R. Grzywacz *et al.*, Phys. Rev. C **100**, 034315 (2019)
[31] R. M. Clark, A. O. Macchiavelli, H. L. Crawford *et al.*, Phys. Rev. C **101**, 034313 (2020)
[32] F. Mercier, J. Zhao, R.-D Lasseri *et al.*, Phys. Rev. C **102**, 011301 (2020)
[33] S. N. Liddick, R. Grzywacz, C. Mazzocchi *et al.*, Phys. Rev. Lett. **97**, 082501 (2006)
[34] K. Auranen, D. Seweryniak, M. Albers *et al.*, Phys. Rev. Lett. **121**, 182501 (2018)
[35] P. Arthuis, C. Barbieri, M. Vorabbi *et al.*, Phys. Rev. Lett. **125**, 182501 (2020)
[36] Satish Kumar and Raj K. Gupta, Phys. Rev. C **49**, 1922-1926 (1994)
[37] Satish Kumar, Dharam Bir, and Raj K. Gupta, Phys. Rev. C **51**, 1762-1771 (1995)
[38] A. Florescu and A. Insolia, Phys. Rev. C **52**, 726-732 (1995)
[39] H. F. Zhang, J. M. Dong, G. Royer *et al.*, Phys. Rev. C **80**, 037307 (2009)
[40] H. Schatz, A. Aprahamian, J. Görres *et al.*, Phys. Rep. **294**(4), 167-263 (1998)
[41] H. Schatz, A. Aprahamian, V. Barnard *et al.*, Phys. Rev. Lett. **86**, 3471-3474 (2001)
[42] Ronald D. Macfarlane and Antti Siivola, Phys. Rev. Lett. **14**, 114-115 (1965)
[43] Chang Xu and Zhongzhou Ren, Phys. Rev. C **76**, 027303 (2007)
[44] Dongdong Ni and Zhongzhou Ren, Phys. Rev. C **80**, 014314 (2009)
[45] Dongdong Ni and Zhongzhou Ren, Nucl. Phys. A **834**, 370c-373c (2010)
[46] Y. Z. Wang, J. Z. Gu, and Z. Y. Hou, Phys. Rev. C **89**, 047301 (2014)
[47] Y. Z. Wang, Z. Y. Li, G. L. Yu *et al.*, J. Phys. G **41**(5), 055102 (2014)
[48] W. M. Seif, M. Ismail, and E. T. Zeini, J. Phys. G **44**(5), 055102 (2017)
[49] National Nuclear Data Center, URL: https://www.nndc.bnl.gov/
[50] L. Capponi, J. F. Smith, P. Ruotsalainen *et al.*, Phys. Rev. C **94**, 024314 (2016)
[51] R. D. Page, P. J. Woods, R. A. Cunningham *et al.*, Phys. Rev. C **49**, 3312-3315 (1994)
[52] C. Mazzocchi, Z. Janas, L. Batist *et al.*, Phys. Lett. B **532**(1), 29-36 (2002)
[53] D. Schardt, R. Kirchner, O. Klepper *et al.*, Nucl. Phys. A **326**(1), 65-82 (1979)
[54] F. Heine, T. Faestermann, A. Gillitzer *et al.*, Z. Phys. A **340**, 225-226 (1991)
[55] D. Schardt, T. Batsch, R. Kirchner *et al.*, Nucl. Phys. A **368**(1), 153-163 (1981)
[56] D. De Frenne and A. Negret, Nucl. Data Sheets **109**(4), 943-1102 (2008)
[57] G. Audi, F. G. Kondev, Meng Wang *et al.*, Chin. Phys. C **41**(3), 030001 (2017)
[58] W. J. Huang, G. Audi, Meng Wang *et al.*, Chin. Phys. C **41**(3), 030002 (2017)
[59] Meng Wang, G. Audi, F. G. Kondev *et al.*, Chin. Phys. C **41**(3), 030003 (2017)
[60] G Royer, J. Phys. G **26**(8), 1149-1170 (2000)
[61] Hongfei Zhang, Wei Zuo, Junqing Li *et al.*, Phys. Rev. C **74**, 017304 (2006)
[62] H. F. Zhang and G. Royer, Phys. Rev. C **76**, 047304 (2007)
[63] G. Royer and H. F. Zhang, Phys. Rev. C **77**, 037602 (2008)
[64] Y. Z. Wang, H. F. Zhang, J. M. Dong *et al.*, Phys. Rev. C

79, 014316 (2009)
[65] H. F. Zhang and G. Royer, Phys. Rev. C **77**, 054318 (2008)
[66] Jun-Gang Deng and Hong-Fei Zhang, Phys. Rev. C **102**, 044314 (2020)
[67] J. M. Dong, H. F. Zhang, and G. Royer, Phys. Rev. C **79**, 054330 (2009)
[68] X. J. Bao, H. F. Zhang, B. S. Hu *et al*., J. Phys. G **39**(9), 095103 (2012)
[69] G. Royer and B. Remaud, Nucl. Phys. A **444**(3), 477-497 (1985)
[70] G. Royer and K. Zbiri, Nucl. Phys. A **697**(3), 630-638 (2002)
[71] Jun-Gang Deng and Hong-Fei Zhang, Phys. Lett. B **816**, 136247 (2021)
[72] H. F. Zhang, G. Royer, and J. Q. Li, Phys. Rev. C **84**, 027303 (2011)
[73] G. L. Zhang, X. Y. Le, and H. Q. Zhang, Phys. Rev. C **80**, 064325 (2009)
[74] Jun-Gang Deng, Jun-Hao Cheng, Bo Zheng *et al*., Chin. Phys. C **41**(12), 124109 (2017)
[75] Jun-Gang Deng, Jie-Cheng Zhao, Jiu-Long Chen *et al*., Chin. Phys. C **42**(4), 044102 (2018)
[76] Ning Wang, Min Liu, Xizhen Wu *et al*., Phys. Lett. B **734**, 215-219 (2014)
[77] Saad M Saleh Ahmed, Redzuwan Yahaya, Shahidan Radiman *et al*., J. Phys. G **40**(6), 065105 (2013)
[78] M. Hasegawa and K. Kaneko, Nucl. Phys. A **748**(3), 393-401 (2005)
[79] Xiao-Dong Sun, Ping Guo, and Xiao-Hua Li, Phys. Rev. C **94**, 024338 (2016)
[80] Jun-Gang Deng, Jie-Cheng Zhao, Dong Xiang *et al*., Phys. Rev. C **96**, 024318 (2017)
[81] Jun-Gang Deng, Jie-Cheng Zhao, Peng-Cheng Chu *et al*., Phys. Rev. C **97**, 044322 (2018)
[82] Chang Xu and Zhongzhou Ren, Phys. Rev. C **69**, 024614 (2004)